Supplementary Material

Golgi enlargement in Arf-depleted yeast cells is due to altered dynamics of cisternal maturation

Madhura Bhave, Effrosyni Papanikou, Prasanna Iyer, Koushal Pandya, Bhawik Kumar Jain, Abira Ganguly, Chandrakala Sharma, Ketakee Pawar, Jotham Austin II, Kasey J. Day, Olivia W. Rossanese, Benjamin S. Glick, and Dibyendu Bhattacharyya

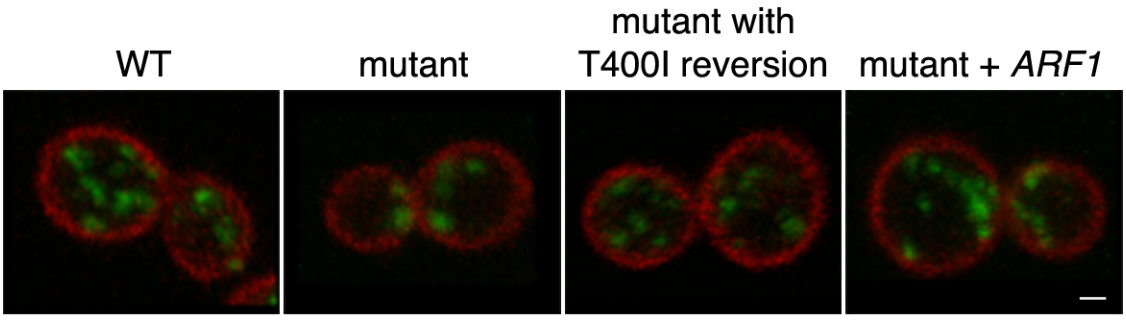

Fig. S1. Reversion or suppression of the *nmt1* mutation restores the wild-type appearance of late Golgi cisternae.

The methods and terminology are as in Fig. 1. Scale bar, 1 μm.

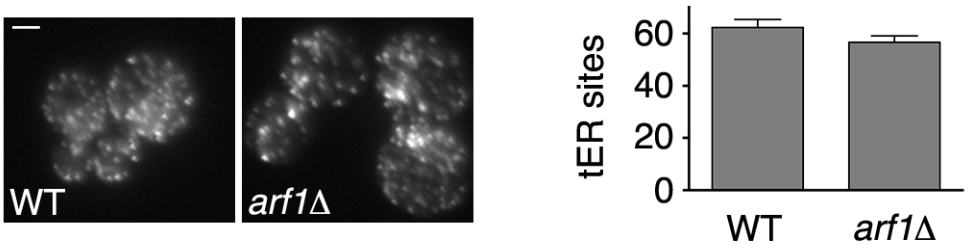

Fig. S2. The *arf1Δ* mutation does not promote tER site coalescence.

Wild-type (WT) or *arf1*Δ cells expressing the tER site marker Sec13-GFP were imaged by fluorescence microscopy. *Left:* representative cells are shown. Scale bar, 2 μm. *Right:* the average number of tER sites per cell was quantified for 25-30 cells from each strain. Error bars indicate s.e.m.

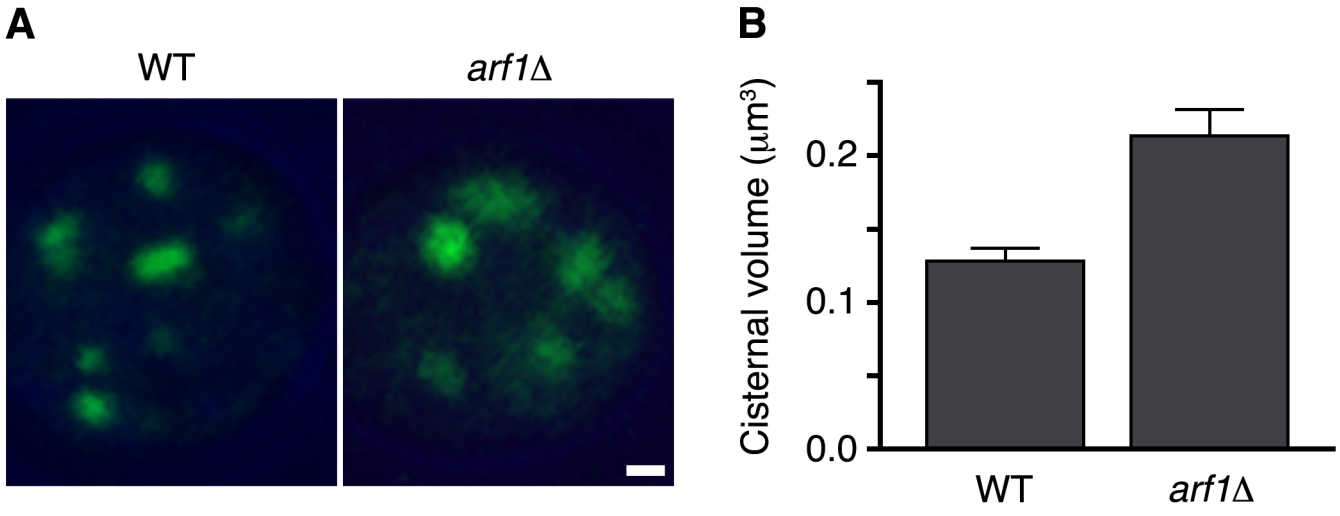

Fig. S3. The *arf1Δ* mutation has only a modest effect on early Golgi cisternae. (**A**) Fluorescence images show representative wild-type (WT) and *arf1Δ* cells expressing GFP-Vrg4. Scale bar, 1 μm. (**B**) The average volume of early Golgi cisternae was measured as in Fig. 1 for WT and *arf1Δ* strains.

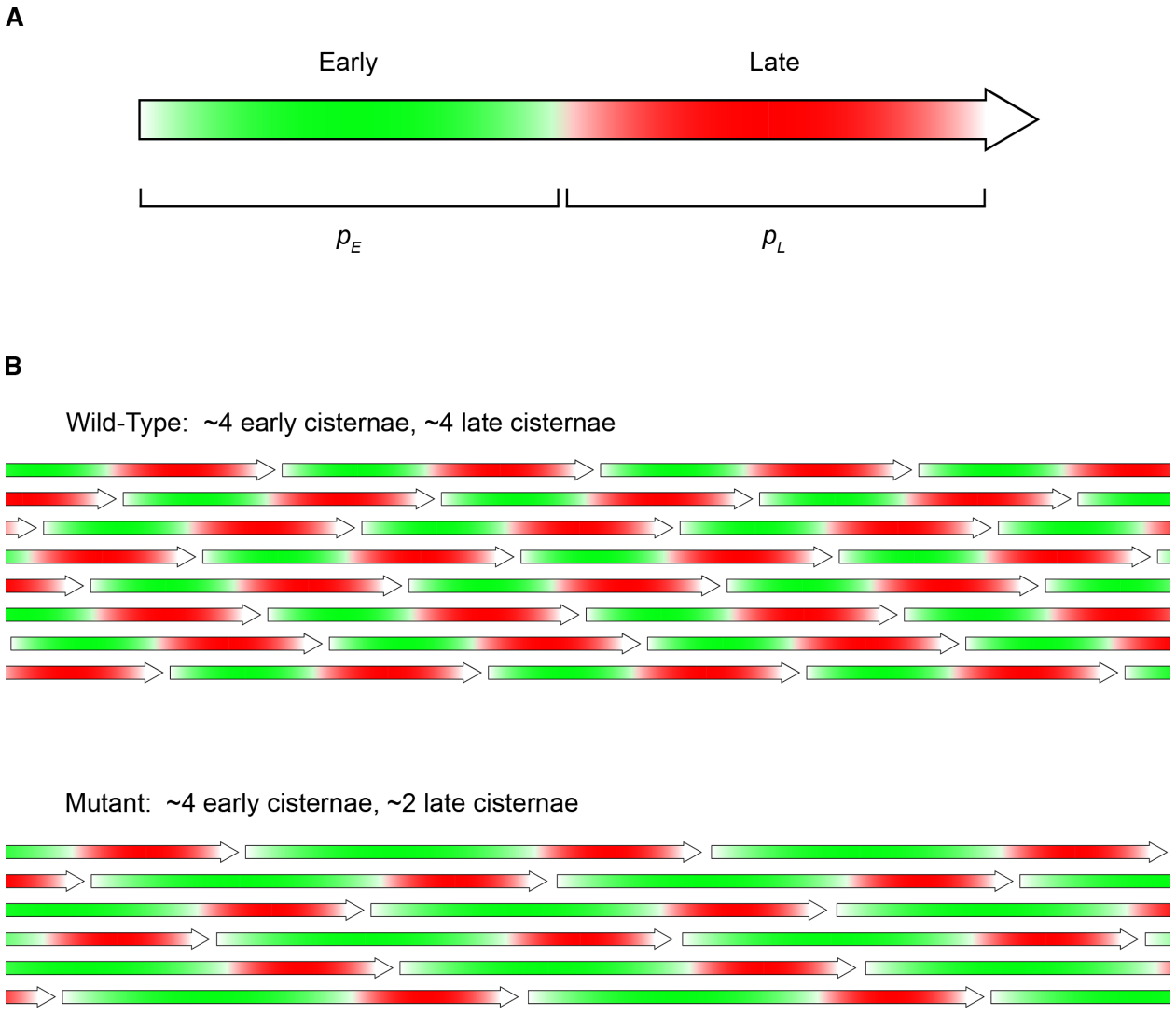

Fig. S4. Graphical representation of the Golgi cisternal life cycle in wild-type and *arf1Δ* cells.

(**A**) Time arrow depiction of a yeast Golgi cisterna, with brackets marking the early Golgi persistence time p_E and the late Golgi persistence time p_L.

(**B**) Simplified model of Golgi cisternal cycles in a wild-type cell and an *arf1Δ* cell. Time proceeds along the horizontal axis, and each arrow represents a different cisterna. Compared to the wild-type cell, the *arf1Δ* cell has twice as large a value of p_E and half as large a value of the maturation frequency m. At any given time point, the *arf1Δ* cell has about the same number of early Golgi cisternae as the wild-type cell but only about half as many late Golgi cisternae. Although this model does not capture the full complexity of Golgi maturation in wild-type and *arf1Δ* cells, it conveys the key insights described in this study.

Movie 1.

Movie 2.

Movie 3.

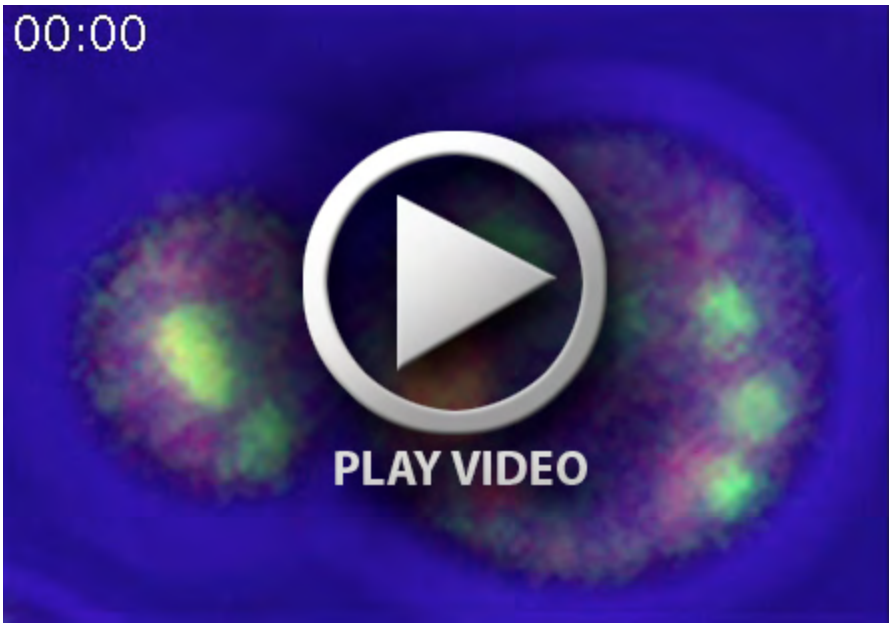

Movie 4.

Movie 1. Tomographic models of late Golgi cisternae in wild-type cells.

Models generated as described in Fig. 2D were assembled using IMOD software (http://bio3d.colorado.edu/imod/) and animated using ImageJ. The models show portions of three late Golgi cisternae from a single thick section.

Movies 2 and 3. Tomographic models of late Golgi cisternae in *arf1*Δ cells.

The procedure was the same as in Movie 1. Movie 2 corresponds to the bottom panels of Fig. 2D, and Movie 3 shows two additional cisternae from a different cell.

Movie 4. Golgi maturation and homotypic fusion in an *arf1*Δ cell.

Early Golgi cisternae were tagged with GFP-Vrg4, and late Golgi cisternae were tagged with Sec7-DsRed. A representative cell was imaged by 4D confocal microscopy with a Zeiss LSM 780 for 3.5 min, with Z-stacks collected at 3.65-sec intervals. Times are indicated in min:sec format, rounded down to the nearest second. In Fig. 4A, frames from this movie illustrate the homotypic fusion of two early Golgi cisternae.